Enhancing GNSS-Based Vehicle Positioning Using DSRC and a Nonlinear Robust Filter under the Connected Vehicles Environment

Liu Jiang*, Cai Bai-gen, and Wang Jian

School of Electronic and Information Engineering, Beijing Jiaotong University,
Beijing 100044, China
Beijing Key Laboratory for Cooperative Vehicle Infrastructure Systems and Safety Control,
Beijing 100191, China
jiangliu@bjtu.edu.cn

Abstract. The concept of IOV (Internet of Vehicles) is capable of ensuring the safety and efficiency in road transportation by using wireless communication among the vehicles and the infrastructure facilities. Precise and real-time positioning of vehicles in the road net is of great significance for many intelligent functions and applications. In this paper, we expand the capability of Dedicated Short Range Communication (DSRC) devices to enhance the GNSS (Global Navigation Satellite System) for vehicle positioning. By utilizing the Huber-based M-estimation technique, an improved robust cubature filter is proposed with a novel approach for real-timely updating the measurement covariance, and a strategy for tuning the filter parameter is designed to improve the adaptability. Simulation results with specific tools show that the robustness and estimation precision of information fusion for positioning can be improved under the uncertain measurement and operating conditions.

1 Introduction

Due to the developing requirements for transportation in nowadays, the mobility, sustainability and safety of road transportation systems have been critical topics of interests all over the world [1]. The concept of Internet of Vehicles (IOV) has been an important part of future intelligent transportation and the realization of the wisdom city, which envisages the vehicles and the objects of the transportation infrastructure are all connected as an internet-based system that is capable of exchanging information for achieving a more efficient, safe and green world of transportation [2]. For lots of IOV applications, vehicle positioning is of great significance for providing fundamental information to support decision-making and further functions.

Traditionally, using the satellite navigation has been a common approach to solve the vehicle location detection issues with a relatively low cost, where the rapid developing GNSSs (Global Navigation Satellite Systems), including GPS, GLONASS

* Corresponding author.

R.C.-H. Hsu and W. Shangguang (Eds.): IOV 2014, LNCS 8662, pp. 110–119, 2014.

and BDS (BeiDou Navigation Satellite System), are strengthening the belief of the users. In order to compensate the drawbacks of GNSS positioning, especially the service unavailability and performance consistency in complex urban environments, many solutions and strategies have been proposed [3~5]. Compared with the sensor-assisted solutions, the wireless communication promotes a novel information resource for enhancing the satellite-based vehicle positioning. DSRC (Dedicated Short Range Communication) based inter-vehicle communication is also involved in the vehicle positioning solution, which uses the Carrier Frequency Offset (CFO) measurements to extend the information used for position computation and is with great potential for assisting the GNSS [6]. In order to make good use of the advantages of GNSS/DSRC integration, the position information processing logic employed in the integrated system has to deal with the problems of nonlinearity in system and measurement model, and uncertain interference in practical operation conditions. The conventional nonlinear filters mainly focus on the nonlinearity approximation capability. However, the deviation between the assumed posterior density and the practical features may result in failures of the connected vehicles services and even greatly rein the availability for some vehicle safety critical applications.

In this paper, we focus on the improvement of the nonlinear filter using the M-estimation technique [7]. A novel nonlinear filtering-based solution is proposed and applied to enhance the performance of GNSS/DSRC positioning, and simulations are carried out to illustrate the performance of the proposed method.

2 Improved Huber-Based Robust Filtering

As many other Bayesian filters, the CKF consists of time update and the measurement update equations. By using the cubature rule, a set of cubature points is involved to solve the nonlinearity in system and measurement models. Consider the discrete-time nonlinear dynamic process:

$$\begin{cases} \boldsymbol{x}_{k+1} = f_k(\boldsymbol{x}_k, \boldsymbol{v}_k) \\ z_k = h_k(\boldsymbol{x}_k, \boldsymbol{w}_k) \end{cases} \tag{1}$$

where $\boldsymbol{x}_k$ is the n -dimensional state vector, z_k is the p -dimensional measurement vector, $f_k(*)$ and $h_k(*)$ are system and measurement functions, $\boldsymbol{v}_k$ and $\boldsymbol{w}_k$ are the system process and the measurement noise vectors, which are assumed fulfilling

$$\mathrm{E}[\boldsymbol{v}_i \boldsymbol{v}_j^{\mathrm{T}}] = \delta_{ij}\boldsymbol{Q}_i, \mathrm{E}[\boldsymbol{w}_i \boldsymbol{w}_j^{\mathrm{T}}] = \delta_{ij}\boldsymbol{R}_i, \mathrm{E}[\boldsymbol{v}_i \boldsymbol{w}_j^{\mathrm{T}}] = 0, \qquad \forall i, j \tag{2}$$

According to standard CKF [**8**], the cubature point set $\{\xi_i, \omega_i\}$ is designed as:

$$\xi_i = \sqrt{m/2}\,[1]_i, \omega_i = 1/m, m = 1, 2, \cdots, m = 2n \tag{3}$$

The state is estimated and the corresponding error covariance is derived as:

$$\hat{\boldsymbol{x}}_k = \hat{\boldsymbol{x}}_{k|k-1} + \boldsymbol{K}_k(\boldsymbol{z}_k - \hat{\boldsymbol{z}}_{k|k-1}) \tag{4}$$

$$\boldsymbol{P}_k = \boldsymbol{P}_{k|k-1} - \boldsymbol{K}_k \boldsymbol{P}_{\mathrm{zz},k|k-1} \boldsymbol{K}_k^{\mathrm{T}} \tag{5}$$

where $\hat{\boldsymbol{x}}_{k|k-1}$ is the state prediction, $\boldsymbol{K}_k$ is the filtering gain, $\boldsymbol{z}_k$ is the measurement vector with its estimation $\hat{\boldsymbol{z}}_{k|k-1}$, $\boldsymbol{P}_{k|k-1}$ is the covariance of prediction, and $\boldsymbol{P}_{\mathrm{zz},k|k-1}$ denotes the innovation covariance matrix.

In the design of the original CKF algorithm, the nonlinearity is highly concerned to achieve an effective solution for the Bayesian filtering scheme. However, since the posterior density is assumed with a fixed form, there are limitations for its nonlinearity approximation capability, especially when the deviations from the assumption exist and the property of interferences is uncertain and complicated due to the operation environments. Therefore, the improvement of robustness is of great necessity in many applications with certain critical performance requirements. By applying the Huber technique, the measurement process of a Bayesian filter can be modified for realizing a Huber-based robust cubature Kalman filter (HRCKF).

With the consideration of the process-based HRCKF approach, the measurement equation can be approximated by integrating the measurement prediction result and the transformed prediction error, which is expressed as:

$$\boldsymbol{z}_k \simeq \hat{\boldsymbol{z}}_{k|k-1} + \boldsymbol{H}_k \boldsymbol{r}_k = \hat{\boldsymbol{z}}_{k|k-1} + \boldsymbol{H}_k(\boldsymbol{x}_k - \hat{\boldsymbol{x}}_{k|k-1}) \tag{6}$$

Thus, the measurement update can be changed to a linear regression problem:

$$\begin{aligned} &\boldsymbol{y}_k = \boldsymbol{\Phi}_k \boldsymbol{x}_k + \boldsymbol{\xi}_k \\ &\rightarrow \boldsymbol{M}_k^{-\frac{1}{2}} \begin{bmatrix} \boldsymbol{z}_k - \hat{\boldsymbol{z}}_{k|k-1} + \boldsymbol{H}_k \hat{\boldsymbol{x}}_{k|k-1} \\ \hat{\boldsymbol{x}}_{k|k-1} \end{bmatrix} = \boldsymbol{M}_k^{-\frac{1}{2}} \begin{bmatrix} \boldsymbol{H}_k \\ \boldsymbol{I} \end{bmatrix} \boldsymbol{x}_k + \boldsymbol{M}_k^{-\frac{1}{2}} \begin{bmatrix} \boldsymbol{w}_k \\ -\boldsymbol{r}_k \end{bmatrix} \end{aligned} \tag{7}$$

where $\boldsymbol{M}_k = diag\{\boldsymbol{R}_k, \boldsymbol{P}_{k|k-1}\}$.

According to the principle of the robust M-estimation, the measurement update is enhanced with a minimization target for a cost function [9]:

$$J(\boldsymbol{x}_k) = \sum_{i=1}^{n} \rho(\Delta_i) \tag{8}$$

where Δ_i represents the i th component of the vector as $(\boldsymbol{\Phi}_k \boldsymbol{x}_k - \boldsymbol{y}_k)_i$, and $\rho(*)$ depicts the Huber's score function that is defined with an adjusting parameter γ [10]

$$\rho(\Delta_i) = \begin{cases} \frac{1}{2}\Delta_i^2, & |\Delta_i| < \gamma \\ \gamma|\Delta_i| - \frac{1}{2}\gamma^2, & |\Delta_i| \geq \gamma \end{cases} \tag{9}$$

In order to obtain a direct solution of the modified filtering with the cost function, it is expected that $J^{'}(\boldsymbol{x}_k) = 0$, and the solution for $\hat{\boldsymbol{x}}_k$ is achieved using the matrix $\boldsymbol{\Theta} = \mathrm{diag}[\psi(\Delta_i)]$, $\psi(\Delta_i) = \rho^{'}(\Delta_i) / \Delta_i$, which means the estimation is solved by

$$\hat{\boldsymbol{x}}_k^{(j+1)} = (\boldsymbol{\Phi}_k^{\mathrm{T}} \boldsymbol{\Theta}^{(j)} \boldsymbol{\Phi}_k)^{-1} \boldsymbol{\Phi}_k^{\mathrm{T}} \boldsymbol{\Theta}^{(j)} \boldsymbol{y}_k, \boldsymbol{P}_k = (\boldsymbol{\Phi}_k^{\mathrm{T}} \boldsymbol{\Theta} \boldsymbol{\Phi}_k)^{-1} \tag{10}$$

where j represents the number of iteration step, and the initial value $\boldsymbol{x}_k^{(0)}$ is derived as $\hat{\boldsymbol{x}}_k^{(0)} = (\boldsymbol{\Phi}_k^{\mathrm{T}} \boldsymbol{\Phi}_k)^{-1} \boldsymbol{\Phi}_k^{\mathrm{T}} \boldsymbol{y}_k$.

With a proper parameter γ, the measurement update process of standard CKF can be replaced, and the Huber function can contribute the robustness capability with its segmentation features. It can be found that the matrix $\boldsymbol{\Theta}$ is actually an integration of two components corresponding to the measurement prediction residual and the state prediction error. If we transform $\boldsymbol{\Theta}$ to be an integration of four parts as:

$$\boldsymbol{\Theta} = \begin{bmatrix} \underset{p \times p}{\boldsymbol{\Theta}_{\mathrm{z}}} & \underset{p \times n}{\boldsymbol{0}} \\ \underset{n \times p}{\boldsymbol{0}} & \underset{n \times n}{\boldsymbol{\Theta}_{\mathrm{x}}} \end{bmatrix} \tag{11}$$

Since the true state is unknown in practical problems, the prediction error is set to zero and thus $\boldsymbol{\Theta}_{\mathrm{x}} = \boldsymbol{0}$. If we introduce Eq. (11) into Eq. (10), it can be derived that the state estimation returns to a standard Kalman filtering form [11]. When we substitute $\boldsymbol{\Theta}_{\mathrm{x}} = \boldsymbol{0}$ into the expressions, the filtering process is given as:

$$\boldsymbol{P}_k = [\boldsymbol{I} - \tilde{\boldsymbol{K}}_k \boldsymbol{H}_k] \tilde{\boldsymbol{P}}_{k|k-1} = [\boldsymbol{I} - \tilde{\boldsymbol{K}}_k \boldsymbol{H}_k] \boldsymbol{P}_{k|k-1} \tag{12}$$

where $\tilde{\boldsymbol{P}}_{k|k-1} = \boldsymbol{P}_{k|k-1}^{1/2} \boldsymbol{\Theta}_{\mathrm{x}}^{-1} (\boldsymbol{P}_{k|k-1}^{1/2})^{\mathrm{T}} = \boldsymbol{P}_{k|k-1}$, and hence $\tilde{\boldsymbol{K}}_k$ is the reweighted Kalman gain that is written as $\tilde{\boldsymbol{K}}_k = \boldsymbol{P}_{k|k-1} \boldsymbol{H}_k^{\mathrm{T}} [\boldsymbol{H}_k \boldsymbol{P}_{k|k-1} \boldsymbol{H}_k^{\mathrm{T}} + \boldsymbol{R}_k^{1/2} \boldsymbol{\Theta}_{\mathrm{x}}^{-1} (\boldsymbol{R}_k^{1/2})^{\mathrm{T}}]^{-1}$. And the state vector will be estimated as:

$$\hat{\boldsymbol{x}}_k = \hat{\boldsymbol{x}}_{k|k-1} + \tilde{\boldsymbol{K}}_k [z_k - h_k(\hat{\boldsymbol{x}}_{k|k-1})] \tag{13}$$

From the results, it is obvious that the matrix $\boldsymbol{\Theta}$ used in the Huber-based filtering just affects the measurement component, where the conventional measurement error covariance is modified to be $\boldsymbol{R}_k^{1/2} \boldsymbol{\Theta}_{\mathrm{x}}^{-1} (\boldsymbol{R}_k^{1/2})^{\mathrm{T}}$. Therefore, it is naturally considered that the enhancement of robustness can be realized by improving only the measurement related component. The covariance $\boldsymbol{M}_k$ will be further enhanced with $\boldsymbol{\Theta}$ as

$$\tilde{\boldsymbol{M}}_k = \boldsymbol{M}_k^{1/2} \boldsymbol{\Theta}^{-1} (\boldsymbol{M}_k^{1/2})^{\mathrm{T}} \tag{14}$$

According to the same reason that mentioned in Eq. (11), the state prediction error is assumed zero so that the improved measurement error covariance $\tilde{\boldsymbol{R}}_k$ is updated by extracting the corresponding components from $\tilde{\boldsymbol{M}}_k$. Based on that, the robustness can be improved by a novel strategy that updates the measurement covariance in standard CKF, rather than the reweighted least-square solution as Eq. (10).

Since the statistical features of the errors cannot accurately described by a certain known distribution, the value of γ will directly affect the performance of nonlinear estimation. In the improved RCKF approach, with an initial γ_0, a simple adjusting strategy is involved to increase the adaptability of the filter. We define a time-varying parameter η_k referring to the discrepancy status of the state prediction and the final estimation, which is described as

$$\begin{aligned} \eta_k &= \chi_k - \chi_{k-1} \\ \chi_k &= (\hat{\boldsymbol{x}}_k - \hat{\boldsymbol{x}}_{k|k-1})^{\mathrm{T}} (\hat{\boldsymbol{x}}_k - \hat{\boldsymbol{x}}_{k|k-1}) \end{aligned} \tag{15}$$

where $\eta_k > 0$ illustrates the strong effect of calibration to the model-based prediction compared to the previous iteration, which requires an enhanced concentration to the filtering performance of the robust method. Therefore, we consider employing a large γ_k in the case of $\eta_k > 0$. An adaptive logic for selecting γ_k is proposed as

$$\gamma_k = \gamma_{k-1} + \omega_0 \eta_k \tag{16}$$

where ω_0 is a fixed scale factor for tuning the adjusting capability of η_k.

3 Application in GNSS/DSRC Vehicle Positioning

In GNSS/DSRC integrated vehicle positioning system, the measurement information from the on-board sensors can be collected and used for the data fusion logic. The architecture of sensor collecting and information fusion is described as Fig.1.

The on-board GNSS receiver obtains the pseudo range from the available satellites. With a different information awareness method, the range (also range rate) between a DSRC transmitter in a neighborhood vehicle and a DSRC receiver within an objective vehicle can be measured based on the Doppler Effect.

According to the principle of sensor measuring for GNSS and DSRC, the proposed filtering-based sensor information fusion will be performed, for which the most decisive step is to set up the system and measurement model as the form in Eq. (1). The three-dimensional position and the related components are involved to make the definition for state vector as $\boldsymbol{x}_k = (x_k, \dot{x}_k, \ddot{x}_k, y_k, \dot{y}_k, \ddot{y}_k, z_k, \dot{z}_k, \ddot{z}_k)^{\mathrm{T}}$.

For the generation of the system kinematical model, with the consideration of implementing a robust estimator, the simple conventional constant acceleration model is sufficient to describe the short-term state transition from instant $(k-1)$ to k.

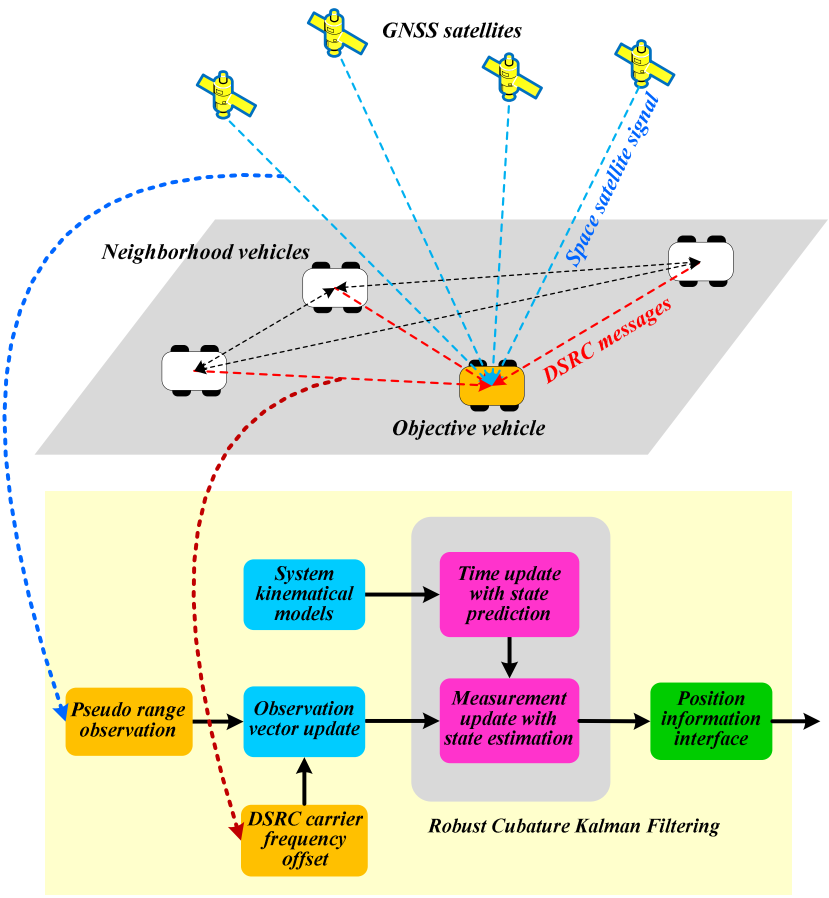

Fig. 1. Architecture of the GNSS/DSRC vehicle positioning system

By this approach, the nonlinear system function $f_k = (*)$ is replaced by a linear state transition process $\boldsymbol{x}_k = \boldsymbol{F}_{k,k-1}\boldsymbol{x}_k + \boldsymbol{v}_k$ with the state transition matrix $\boldsymbol{F}_{k,k-1}$.

For the measurement process, at a certain time instant k, the observations from n_s GNSS satellites and n_d neighborhood vehicle nodes are combined to update the measurement vector z_k. It can be seen that the measurements from two positioning systems are integrated with a tightly coupled architecture, where the observations are combined to achieve a complete calculation solution for vehicle position estimation. With the definitions of the system model $\boldsymbol{F}_{k,k-1}$ and measurement model $h_k(*)$, the integration of GNSS and DSRC can be performed according to the proposed robust filtering algorithm, and the performance of vehicle positioning will be improved than the conventional filters, especially the capabilities under uncertain conditions.

4 Simulation Analysis and Discussion

We present our simulation results to validate the proposed improved robust cubature Kalman filter for the GNSS/DSRC vehicle positioning problem. We generate a traffic simulation scenario, where a local road network is built covering totally 9 signalized intersections. The traffic flow is generated according to a pre-defined OD condition, where the dynamic state of the simulated vehicles is recorded real-timely using corresponding APIs. An objective vehicle (OV) is tracked based on its ID and the DSRC measurements from its neighborhood vehicles (NVs) are simulated, where the effective communication coverage is set with a radius of 150m and the measurement error of DSRC increases with V2V relative distance. Fig.2 shows the road network in simulation and indicates the situation of OV and NVs at the time instant $t = 66s$.

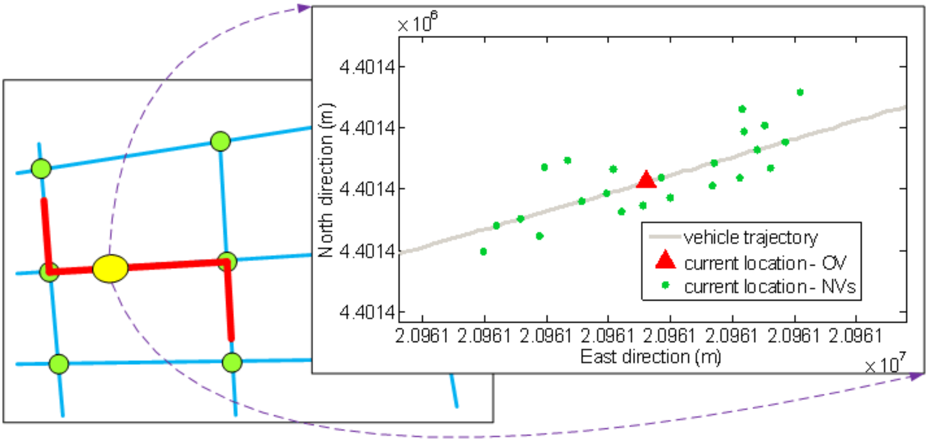

Fig. 2. Vehicle trajectory and the distribution of neighborhood vehicles as t=66s

As presented in the Fig.2, there are 23 neighborhood vehicles travelling within the DSRC coverage of the OV. In positioning calculation for the OV, we use four neighborhood vehicle nodes to update measurement vector in an iteration, according to the relative distance and the space distribution of the NVs, which may influence the communication quality and the dilution of precision for locating the vehicle.

With the extracted trajectory of the OV, the satellite receiver measurement is simulated with a GNSS Simulator. The pseudo-ranges of the BDS satellites are generated according to specific observation models. In order to validate the vehicle positioning performance in the practical environment, the ionospheric delay and tropospheric delay can be coupled in the original observation simulation process, which provides effective conditions for validating the filtering performance.

When using the BDS simulation results under normal conditions, three positioning modes are involved in the comparison to illustrate the performance of IHRCKF, including (1) BDS-based positioning, (2) BDS/DSRC with standard CKF, and (3) BDS/DSRC with the improved IHRCKF method. With the real state of the OV, the positioning errors in both the east and north direction under a Gauss plane coordinate can be calculated. We use RMSE (Root Mean Square Error) to evaluate the filtering precision. Fig.3 and Fig.4 depict the RMSE in east and north directions.

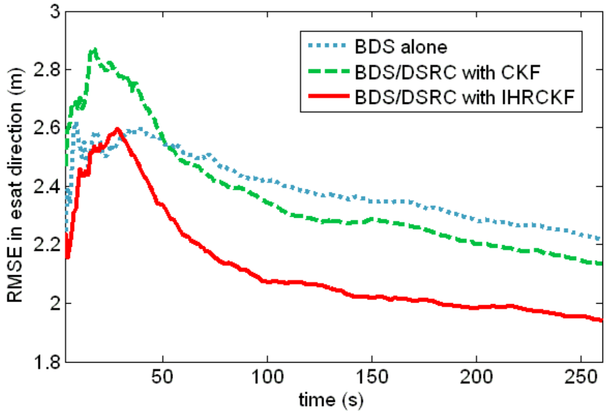

Fig. 3. Comparison of RMSE in east direction with different positioning modes

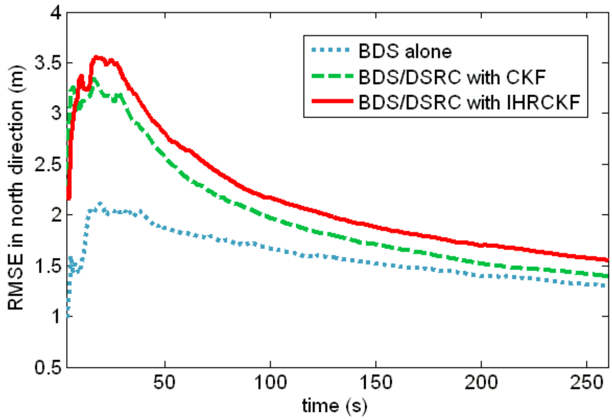

Fig. 4. Comparison of RMSE in north direction with different positioning modes

From the figures, it can be found that, compared to the BDS alone mode and the CKF-based integration mode, the IHRCKF solution contributes certain improvement in positioning precision. However, the performance of the IHRCKF is not enhanced greatly where the BDS is simulated with normal conditions.

In order to validate the effectiveness of the proposed approach, both the CKF and the IHRCKF solutions are involved in simulation with GNSS measurements under the challenging conditions. Different values for diagonal elements of $\boldsymbol{R}_k$ are compared. We use σ_{G} and σ_{D} to indicate the predefined measurement covariance of each satellite and the on-board DSRC device of those related neighborhood vehicles, which means $\boldsymbol{R}_k = diag(\sigma_{\mathrm{G}}^2, \cdots, \sigma_{\mathrm{G}}^2, \sigma_{\mathrm{D}}^2, \cdots, \sigma_{\mathrm{D}}^2)$. A wide range of covariances (from 2.0 to 100.0) for both σ_{G} and σ_{D} are tested.

The results of CKF and IHRCKF are summarized in Table 1 and Table 2, where the deviation between the maximum and minimum RMSE with different σ_{G} values for a certain σ_{D} is calculated and recorded as $\Delta D_{\text{max-min}}$ in the tables. The meaning of $\Delta G_{\text{max-min}}$ can be described with a similar approach. Both the $\Delta D_{\text{max-min}}$ and $\Delta G_{\text{max-min}}$ provide obvious descriptions for evaluating the sensitivity to the different covariance assumption conditions.

Table 1. RMSE and its max-min deviation of CKF with different measurement covariances

σ_{G}	**2.0**	**5.0**	**10.0**	**50.0**	**100.0**
$\Delta G_{\text{max-min}}$	1.0169	0.9601	1.6082	7.2037	14.3639
σ_{D}	**2.0**	**5.0**	**10.0**	**50.0**	**100.0**
$\Delta D_{\text{max-min}}$	4.7672	10.2799	13.1983	1.7245	1.6937

Table 2. RMSE and its max-min deviation of IHRCKF with different measurement covariances

σ_{G}	**2.0**	**5.0**	**10.0**	**50.0**	**100.0**
$\Delta G_{\text{max-min}}$	1.4958	1.1279	1.4836	1.4227	1.6358
σ_{D}	**2.0**	**5.0**	**10.0**	**50.0**	**100.0**
$\Delta D_{\text{max-min}}$	0.9858	0.7852	0.6315	1.7163	2.3167

It can be found that a better robustness performance of state estimation of vehicle positioning is obtained by the proposed IHRCKF. Compared to the results from CKF, the response of IHRCKF to the variety of covariance assumptions is insensitive and relatively stable, while the deviation of CKF is with distinct diversity in a wide range from 1.0169 to 14.3639. It is illustrated that the modification of the measurement covariance in IHRCKF and the adaptive γ strategy greatly enhance the robustness of GNSS/DSRC integration to deal with the unknown error characteristics and operation conditions, while the conventional filtering method that uses a fixed $\boldsymbol{R}_k$ is lack of adaptability and cannot cope with the uncertainties with the specific assumptions.

5 Conclusions

In this paper, we proposed an improved robust cubature Kalman filter to fuse the sensor data for locating the vehicles, using the GNSS/ DSRC positioning scheme. The proposed approach solves the issues of nonlinearity and robustness, and poses problem for the conventional filtering techniques like the cubature Kalman filter and other related solutions. By modifying the measurement process of the standard CKF using an adaptive strategy for measurement covariance matrix and the key parameter

γ, the sensitivity of the estimation precision to the covariance assumptions and the operating conditions is effectively constrained. Simulation results demonstrate the capability of the proposed filter approach, and show its potential for implementation in practical connected vehicles environment.

Acknowledgement. This research was supported by the International Science & Technology Cooperation Program of China (2014DFA80260), Fundamental Research Funds for the Central Universities (2014JBM003), Beijing Natural Science Foundation (4144081), National Natural Science Foundation of China (U1334211, 61273089).

References

1. Lee, J., Park, B.: Development and evaluation of a cooperative vehicle intersection control algorithm under the connected vehicles environment. IEEE Transactions on Intelligent Transportation Systems 13(1), 81–90 (2012)
2. Dimitrakopoulos, G.: Intelligent transportation systems based on internet-connected vehicles: Fundamental research areas and challenges. In: The 11th International Conference on ITS Telecommunications, St. Petersburg, pp. 145–151 (2011)
3. Liu, J., Cui, X., Lu, M., Feng, Z.: Direct position tracking loop based on linearised signal model for global navigation satellite system receivers. IET Radar, Sonar and Navigation 7(7), 789–799 (2013)
4. Sazdovski, V., Silson, P.: Inertial navigation aided by vision-based simultaneous localization and mapping. IEEE Sensor Journal 11(8), 1646–1656 (2011)
5. Wei, L., Cappelle, C., Ruichek, Y.: Camera/laser/GPS fusion method for vehicle positioning under extended NIS-based sensor validation. IEEE Transactions on Instrumentation and Measurement 62(11), 3110–3122 (2013)
6. Alam, N., Balaei, A., Dempster, A.: An instantaneous lane-level positioning using DSRC carrier frequency offset. IEEE Transactions on Intelligent Transportation Systems 13(4), 1566–1575 (2012)
7. Chang, L., Hua, B., Chang, G., Li, A.: Robust derivative-free Kalman filter based on Huber's M-estimation methodology. Journal of Process Control 23(10), 1555–1561 (2013)
8. Arasaratnam, I., Haykin, S.: Cubature Kalman filters. IEEE Transactions on Automatic Control 54(6), 1254–1269 (2009)
9. Wang, X., Cui, N., Guo, J.: Huber-based unscented filtering and its application to vision-based relative navigation. IET Radar, Sonar and Navigation 4(1), 134–141 (2009)
10. Karlgaard, C., Schaub, H.: Huber-based divided difference filtering. Journal of Guidance, Navigation and Control 30(3), 885–891 (2007)
11. Chang, L., Hu, B., Chang, G., Li, A.: Huber-based novel robust unscented Kalman filter. IET Science, Measurement and Technology 6(6), 502–509 (2011)